Optical Materials 50 (2015) 199–203

Contents lists available at ScienceDirect

Optical Materials

journal homepage: www.elsevier.com/locate/optmat

5d–4f emission of Eu^{2+} and electron-vibrational interaction in several alkaline earth sulfides doped with Eu^{2+} and Er^{3+}

G.A. Kumar [a,b,*], D.-X. Liu [c], Y. Tian [c], M.G. Brik [c,d,e,f], D.K. Sardar [a]

[a] Department of Physics and Astronomy, University of Texas at San Antonio, TX 78249, USA
[b] Department of Atomic and Molecular Physics, Manipal University, Manipal 576104, India
[c] College of Sciences, Chongqing University of Posts and Telecommunications, Chongqing 400065, PR China
[d] Institute of Physics, University of Tartu, Ravila 14C, Tartu 50411, Estonia
[e] Institute of Physics, Jan Dlugosz University, PL-42200 Czestochowa, Poland
[f] Institute of Physics, Polish Academy of Sciences, al. Lotników 32/46, 02-668 Warsaw, Poland

ARTICLE INFO

Article history:
Received 20 August 2015
Received in revised form 21 September 2015
Accepted 22 October 2015
Available online 29 October 2015

Keywords:
Photostimulated luminescence
Upconversion
Optical material
Electron–phonon interaction
Huang–Rhys factor

ABSTRACT

Several alkaline earth sulfides doped with Eu^{2+} and Er^{3+} ions have been synthesized and shown to be potential phosphors for applications in the visible spectral range. The excitation and emission spectra corresponding to the 4f–5d interconfigurational transitions of Eu^{2+} were analyzed with an aim of extraction of the main parameters of the electron-vibrational interaction. The values of the Huang–Rhys factor, effective phonon energies, and zero-phonon line positions were systematically compared for all studied materials; physical trends were discussed. As a test for the validity of the obtained parameters, the Eu^{2+} 5d–4f emission bands were modeled to yield good agreement with the experimental spectra.

1. Introduction

Photostimulated luminescence (PSL) is a well studied luminescence phenomena and so many phosphors have been developed over the past. In PSL the emission is due to the recombination of the electrons and hole traps which are created by the high energy radiation sources such as X rays, UV rays, cathode rays, and gamma rays. The depth of the trapping centers are usually large and are in the order of 1–2 eV. At room temperature, the probability of thermal activation of the trapping centers is extremely small and hence the PSL phosphors can serve as excellent data storage materials. The recombination process is induced by the energy supplied to the material in the form of infrared or visible radiations and this result in the emission of light from the activator. Most of the PSL phosphors are wide band gap II–VI semiconductors doped with two types of selected rare earths in divalent and trivalent states.

The applications of PSL phosphors in the Photonics industry and military area are very wide such as optical storage, PSL dosimeters, infrared sensors, image intensifiers, NIR to visible convertors, and tracking of IR sources such as vehicles and missiles [1–5]. These materials also have high quantum conversion efficiency of the order of 66% and short IR response time.

Rare earth doped alkaline earth sulfides are considered as very efficient PSL phosphors [6,7]. Over the past several reports have been published on the synthesis and characterizations of various rare earth doped Ca and Sr sulfide phosphors both in bulk and nano crystalline forms [6–9]. Especially the Eu^{2+} doped SrS and CaS are considered as two of the most efficient red phosphors for LED applications [10]. It was found that the emission color can be considerably shifted by changing the nature of the alkaline earth cation as well as its composition in the crystal lattice. In this paper we report the synthesis and optical characterization of CaS, SrS, CaSrS, CaMgS doped with Eu^{2+} and Er^{3+}. A theoretical model based on the electron–phonon interaction was used to interpret the spectral shift as a function of the cationic compositions.

2. Sample preparation and measurements

All phosphor samples were prepared by the solid state reaction technique in CO reductive atmosphere. The starting raw materials were $CaCO_3$,$SrCO_3$,$(MgCO_3)_4$,Eu_2O_3,Er_2O_3, elemental S, and LiF (Sigma Aldrich, 99.99% pure). Based on published report [11] the

* Corresponding author at: Department of Physics and Astronomy, University of Texas at San Antonio, TX 78249, USA.
E-mail address: ajith@gakumar.net (G.A. Kumar).

http://dx.doi.org/10.1016/j.optmat.2015.10.024
0925-3467/

rare earth dopant concentration was fixed at 0.2 mol% for the best emission intensity. Elemental S is added in excess to compensate the oxidation losses and LiF is added as a flux which is typically 10% of the total weight of the reactants. All the chemicals were mixed in an agate mortar and fired at 1100 °C for 1.25 h and the obtained sample was crushed to obtain the ceramic phosphor sample.

Powder X-ray diffraction was performed at 40 kV and 30 mA in the parallel beam configuration using a RIGAKU Ultima IV X-ray diffractometer with Cu Kα (λ = 1.5 A). The absorption spectra were measured in the 300–1700 nm range using a spectrophotometer (Cary, Model 14R) in transmission mode by mixing the powder sample with epoxy and keeping in between glass slides. The emission spectra of the samples were recorded by exciting the sample with 980 nm band of a Ti:Sapphire laser (Spectra Physics, Model 3900S) pumped by a frequency doubled Nd:YVO_4 laser (Spectra Physics Millennia). The emission from the sample was collected with a 1.25 m single grating scanning monochromator (SPEX, Model 1250 M) and detected by a photo multiplier tube (Model 1911, Horiba) for the visible.

3. Results and analysis of the electron-vibrational interaction

Figs. 1a and 1b show the XRD patterns of the CaS and SrS phosphors in comparison with the standard powder pattern. Both XRD pattern obtained are in agreement with the respective powder standard (JCPDS card no. 75-0895 for SrS, JCPDS card no. 08-0464 for CaS), The room temperature UV–VIS absorption spectrum in Fig. 2) shows two well defined peaks at 250 (Eu^{2+} $^6I_{15/2} \rightarrow {}^8S_{7/2}$) and 543 nm ($Er^{2+}$ $^1G_4 \rightarrow {}^3H_6$) and a very broad NIR band at 1203 nm (Er^{2+} $^3H_5 \rightarrow {}^3H_6$) that extend from 800 to 1600 nm which makes this phosphor for wide excitation range upconversion applications. Upon excitation at 980 nm strong upconversion was observed in the red region and the emission spectra are shown in Figs. 3a–e for various phosphor compositions.

Influence of the lattice vibrations on the impurity ion electron states manifest itself in the shift of the emission band maximum with respect to the maximum of the corresponding absorption band. Such an interaction is more pronounced for open electron shells (like 5d shells of rare-earth ions, for example) and is considerably weaker for inner 4f shells. Quantitatively, interaction between electronic states of an impurity ion and vibrations of ligands is described by the following parameters: the Stokes shift ΔE_S (the difference in energy between the absorption and emission peaks), the Huang–Rhys factor S (which is proportional to ΔE_S) and effective phonon energy $\hbar\omega$. All these parameters can be estimated from a comparative analysis of the emission and absorption (or excitation) spectra. The following equations can be used [12]

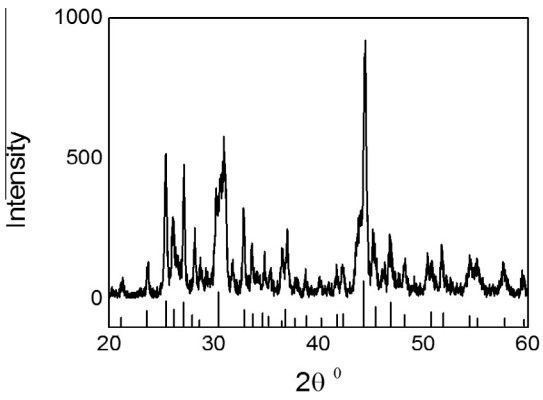

Fig. 1a. XRD pattern of SrS: Eu^{2+}, Er^{3+} in comparison with JCPDS standard 75-0895.

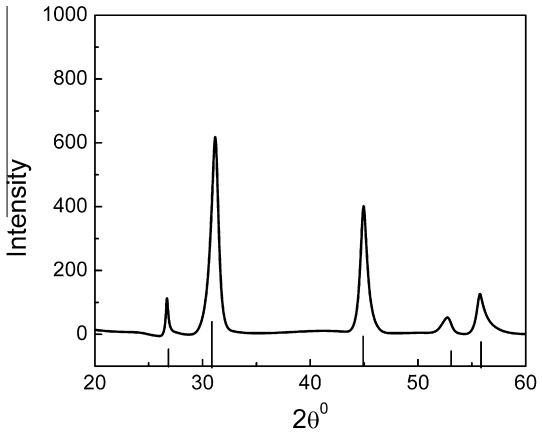

Fig. 1b. XRD pattern of CaS: Eu^{2+}, Er^{3+} in comparison with JCPDS standard 08-0464.

$$\Delta E_S = (2S-1)\hbar\omega, \tag{1}$$

$$\Gamma(T) = 2.35\hbar\omega\left[S\coth\left(\frac{\hbar\omega}{2kT}\right)\right]^{1/2}, \tag{2}$$

where the last equation describes the full width $\Gamma(T)$ at half maximum (FWHM) of the emission band determined at the absolute temperature T.

Before proceeding with applications of Eqs. (1) and (2) to the title systems, we point out here that the Eu^{2+} $4f^7 \rightarrow 4f^65d^1$ absorption (excitation) bands are very broad (Fig. 2). This is related to the crystal field splitting of the Eu^{2+} energy levels. In the sulfides studied in the present work the Eu^{2+} ions occupy the divalent cation positions, which are surrounded by six S^{2-} ions. In the octahedral crystal field the 5d states of Eu^{2+} are split into the t_{2g} (the lowest) and e_g (the highest) levels [13], which can be split further due to the low-symmetry component of crystal field. Then one may expect in general five excitation bands (which can be strongly overlapping) in the excitation spectra. The emission transition will start from the lowest 5*d* level, according to the general shape of the photoluminescence band, which represents a practically Gaussian function with one clearly distinguished maximum and without any additional structure (Fig. 3). The general scheme (not to scale) of the 5d levels splitting with characteristic emission and absorption transitions relevant for the present discussion is shown in Fig. 4.

For each considered host the absorption band corresponding to the t_{2g} states was decomposed into three Gaussian functions, and the position of the longest wavelength maximum was taken as the first absorption transition. Results of application of Eqs. (1) and (2) are summarized in Table 1.

The structure of the absorption spectra of the studied samples clearly reveals presence of two wide bands, which correspond to the transitions from the ground Eu^{2+} state to the t_{2g} (lower in energy band) and e_g (higher in energy band) states, which arise from the crystal field splitting of the 5d states of europium. Separation between the barycenters of this states is the crystal field strength parameter 10*Dq*.

Analysis of the 10*Dq* (5d states splitting) shows that it is maximum for CaS and $Ca_{0.7}Mg_{0.3}S$. With increasing of the Sr content and with gradual move to SrS, the 10*Dq* value is decreasing due to increasing interatomic distances (this trend can be understood by comparing the Sr–S and Ca–S distances in pure materials (3.0095 Å [14] and 2.8452 Å [15], respectively)). In addition, the longest wavelength of the Eu^{2+} emission corresponds to the strongest crystal field (largest 10*Dq* value), whereas the shortest wavelength is related to the weakest crystal field (Table 1),